

# We are IntechOpen, the world's leading publisher of Open Access books Built by scientists, for scientists

6,900

Open access books available

186,000

International authors and editors

200M

Downloads

Our authors are among the

154

Countries delivered to

TOP 1%

most cited scientists

12.2%

Contributors from top 500 universities



WEB OF SCIENCE™

Selection of our books indexed in the Book Citation Index  
in Web of Science™ Core Collection (BKCI)

Interested in publishing with us?  
Contact [book.department@intechopen.com](mailto:book.department@intechopen.com)

Numbers displayed above are based on latest data collected.  
For more information visit [www.intechopen.com](http://www.intechopen.com)



# Develop a Power Detection and Diagnosis Module for Mobile Robots

Kuo-Lan Su<sup>1</sup>, Jr-Hung Guo<sup>2</sup> and Jheng-Shiann Jhuang<sup>3</sup>

<sup>1</sup>*Department of Electrical Engineering, National Yunlin University of Science & Technology, Douliou, Yunlin 640, Taiwan. sukl@yuntech.edu.tw*

<sup>2</sup>*Graduate school Engineering Science and technology National Yunlin University of Science & Technology, Douliou, Yunlin 640, Taiwan, g9710801@yuntech.edu.tw*

<sup>3</sup>*Department of Electrical Engineering, National Yunlin University of Science & Technology, Douliou, Yunlin 640, Taiwan. 9512710@yuntech.edu.tw*

## 1. Abstract

Autonomous mobile robot will be very flexibility to move in free space. But it is limited on power supply. The power of the mobile robot can provide a few hours of peak usage before the power is lack. The power detection system is an important issue in the autonomous mobile robot. In the chapter, we want to design a power detection and diagnosis module to measure the power condition of the mobile robot, and measure the voltage of the power system for mobile robots. We use multilevel multisensory fusion method to detect and diagnose current sensors and voltage signals of mobile robots. First, we use four current sensors to measure the power variety of the mobile robot. We use redundant management method and statistical predition method to detect and diagnosis current sensor status, and isolate faulty sensor to improve the power status to be exact. Then, we use computer simulation to implement the proposed method to be adequate. We design the power detection and diagnosis module using HOLTEK microchip. Users can select maximum and minimum current value and detection range of the power detection module. The power detection module can transmits the detection and diagnosis status to the main controller (Industry Personal Computer, IPC) of the mobile robot via series interface. Finally, we implement some experimental scenario using the module in the mobile robot, and can take some experimental results for some variety condition on sensor faulty.

Keywords - Autonomous mobile robot, redundant management method, statistical perdition method.

## 2. Introduction

With the robotic technologies development with each passing year, Mobile robots have been widely applied in many fields. Such as factory automation, dangerous environment detection, office automation, hospital, entertainment, space exploration, farm automation,

military and security system. Recently more and more researchers take interest in the field especially intelligent service robot. There are some successful examples, ASIMO, KHR, QRIO and AIBO. In our laboratory, we have been designed a mobile robot (ISLR-I) to fight fire source. However the mobile robot has been working for a long time. The power of the mobile robot is lack, and it can not be controlled by the command, and some dangerous event may be happened. Thus, the mobile robot must quickly move to the recharging station. So we must detect power variety of the mobile robot all the time. Therefore, we must detect power variance of the mobile robot very carefully. We must calculate the residual power according to the power output of the mobile robot. The mobile robot has enough time to move to the recharging station autonomously.

We have designed a power detection system in the WFSR-I mobile robot. The contour of the robot is cylinder. The mobile robot has the shape of cylinder and its diameter, height and weight is 20cm, 30cm and 4kg. The robot is a four-wheeled platform equipped with a main controller (MCS-51 microprocessor). The power system of the mobile robot uses two rechargeable batteries [1,2,19]. We use laser line guard the mobile robot move to the recharging station. Next, we modify the power detection module applying in Chung-Cheng I security robot using microprocessor (MCS51), too. The Chung-Cheng I security robot has the shape of cylinder and its diameter, height and weight is 50cm, 150cm and 80kg. The module can calculate the exact current variety of the Chung-Cheng I security robot, and use image guard the security robot move to the recharging station. The experimental results are very successful [3,5]. Now we design the power detection module applying in the ISLR-I mobile robot using HOLTEK microchip. The new module wants to reduce the cost of the power detection module, and extend more and more functions for mobile robots. The module can transmit the power detection results to the main controller of the mobile robot via series interface.

In the past literature, many researches have been proposed current detection methods. A. J. Melia and G.F. Nelson postulate that monitoring of the power supply current could aid in the testing of digital integrated circuits [6,7]. Levi was one of the first to comment upon the characteristics of CMOS technology which make it special amenable to IDD Testing [8]. Malaiy and Su use IDD testing and estimating the effects of increased integration on measurement resolution [9,10]. Frenzel proposed the likelihood ration test method applying on power-supply current diagnosis of VLSI circuits [11]. Horming and Hawkins reported on numerous experiments where current measurements have forecast reliability problems in devices which had previously passed conventional test procedures[12,13]. Then, many researches dedicated to improving the accuracy of measuring current [14,15]. Maly et al proposed a build-in current sensor which provides a pass/fail signal when the current exceeds a set threshold [16,17].

The chapter is organized as follows: Section II describes the system structure of the power detection system for the ISLR-I mobile robot. Section III presents the hardware structure of power detection system for the mobile robot. The detection and diagnosis algorithm is explained in section IV. Section V explains the user interface of the power detection system for the mobile robot. Section VI presents the experimental results for power detection and isolation scenario of mobile robot. Section V presents brief concluding remarks.

### 3. System Architecture

The mobile robot is constructed using aluminium frame. The mobile robot has the shape of cylinder and its diameter, height and weight is 50 cm, 110cm and 40 kg. Figure 1 (a) shows the hardware configuration of the mobile robot (ISLR-I). The main controller of the mobile robot is industry personal computer (IPC). The hardware devices have GSM modem, batteries, NI motion control card, wireless LAN, fire fighting device and sensory circuits, touch screen, distributed control module, power detection and diagnosis module, driver system, DC servomotors, color CCD and some hardware devices [18].

There are six systems in the mobile robot, including structure, avoidance obstacle and driver system, software development system, detection system, remote supervised system and others. Figure 1 (b) is the hierarchy structure of the mobile robot, and each system includes some subsystem. For example, the detection system contains power detection system, fire fighting device, fire detection rule and fire detection hardware... etc.

Manuscript must contain clear answers to following questions: What is the problem / What has been done by other researchers and where you can contribute / What have you done / Which method or tools you used / What are your results / What is new and good, what is not good / Future research.

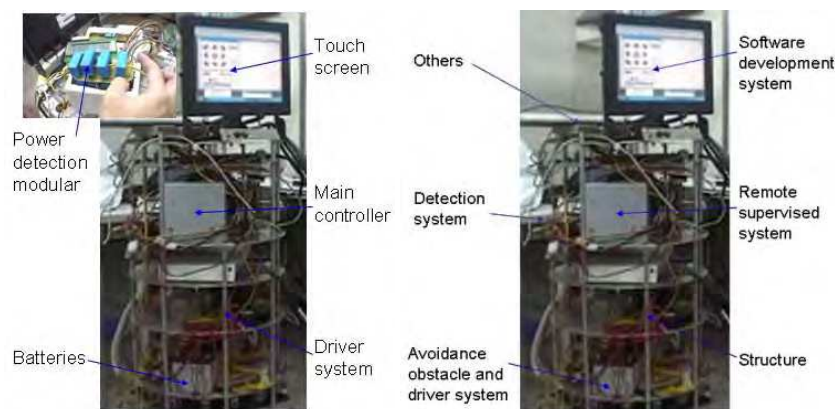


Fig. 1. The contour and structure of the mobile robot (ISLR-I).

### 4. Power Detection System

The power detection system of the mobile robot is shown in Figure 2. We proposed a power detection and diagnosis system using four current measured values and four voltage measured values, and use a multilevel multisensor fusion method to decide the exact power output of mobile robot. The power detection system contains six parts (see Figure 2). They are main computer, auto-switch, A/D and I/O card, the power detection and isolation module, batteries and three detection algorithms. The main computer implements the statistical signal prediction method and polynomial regression algorithm, and control the A/D and I/O card. The A/D and I/O card can control the auto-switch to cut off the power of the mobile robot. The main controller of the mobile robot can calculate power value according the current and voltage measured values. The redundant management method is implemented in the power detection and isolation module.

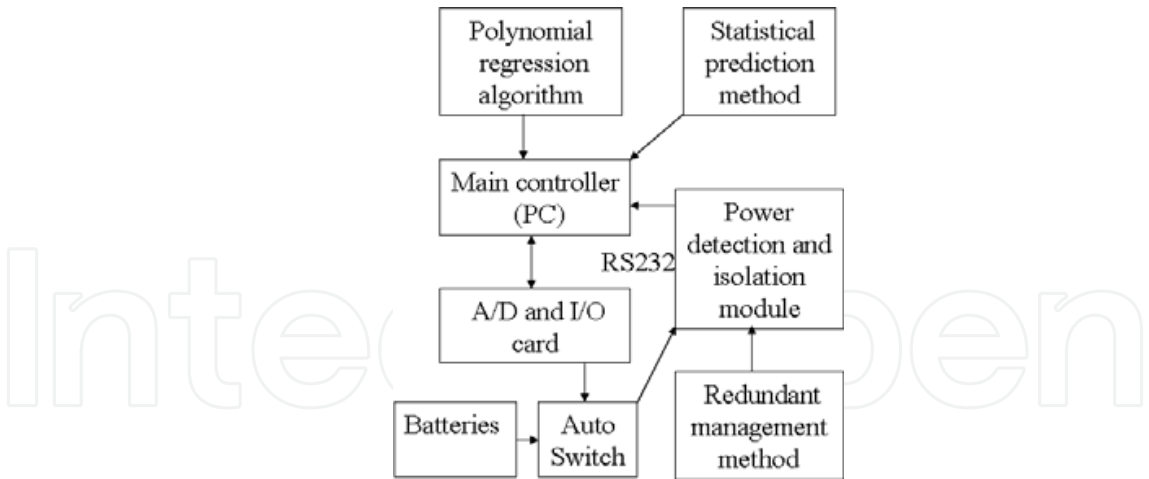


Fig. 2. The power detection and prediction system of the mobile robot

The power detection system of the mobile robot contains four DC type current sensors, a HOLTECK microchip (controller), display and alarm device, some hardware devices and a series interface. The hardware block diagram of the power detection and isolation module is shown in Figure 3. The controller is a HOLTEK microchip (HT46R25), and detects the power variance using four DC type current sensors and voltage measured values. The input signal has scale selection switch and mode selection switch. The output signal contains safety switch, series interface, display and alarm device. The safety switch may be used to turn on or off the power of the mobile robot according to the real status. The power detection module can measure maximum current up to about 50A. The prototype of the power detection, diagnosis and isolation module is shown in Figure 4.

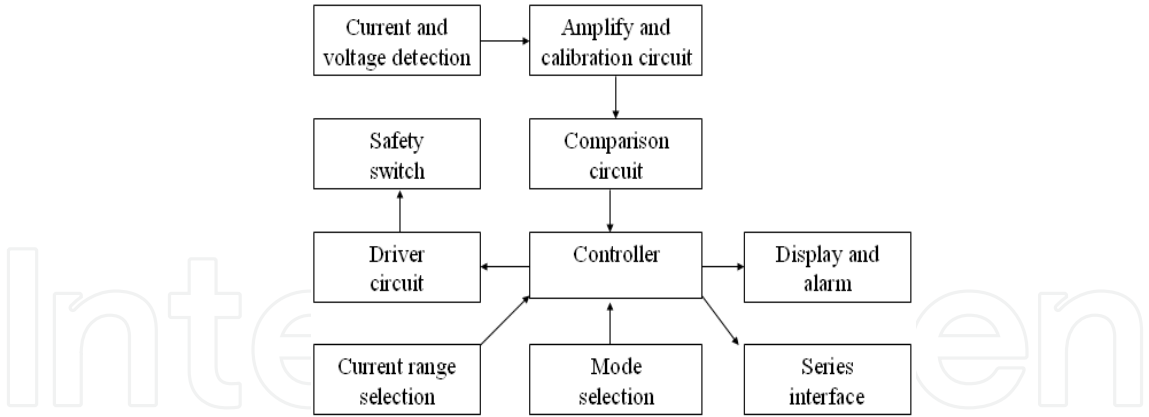


Fig. 3. The hardware block diagram of the power detection module



Fig. 4. The prototype of the power detection module

5. Detection Algorithm

In the power detection, diagnosis and isolation module, we use redundant management method and statistical perdition method to detect and diagnose sensory status and isolate faulty sensors. The redundant measurements of a process variable are defined as [4].

$$M = HX + E$$

$$|\varepsilon_i| \leq b_i$$

- Where:
- M = the measure vector ( 1 x 1) is generated from sensors.
  - H = the measurement matrix ( 1 x n).
  - X = the n-dimensional measured true values.
  - E = the measurement error.
  - $b_i$  = The specified error bound of the measurement  $m_i$

The fault detection and isolation procedure presented in the chapter is applicable to scalar measurements only. The measurement matrix in equation (1) can be chosen as  $H = [1,1,...1]^T$  , without loss of generality. A pair of scalar measurements  $m_i$  and  $m_j$  . The magnitude of  $(m_i - m_j)$  is compared with the sum  $(b_i + b_j)$  of the respective error bounds for a consistency check. Any two scalar measurements  $m_i$  and  $m_j$  at the sample time k are defined to be consisted if

$$|m_i(k) - m_j(k)| \leq (b_i(k) + b_j(k))$$

(3)

Otherwise, we can say the two scalar measurements  $m_i$  and  $m_j$  to be inconsistency. In this condition, the consistency index of a measurement  $m_i$  is defined at a given sample time as

$$I_i = \sum_{j=1}^l f\left[|m_i - m_j| \leq (b_i + b_j)\right] \quad i = 1 \dots l$$

(4)

Where  $l$  sensor numbers and the indicator function are  $f[*]$  to be defined as



$$f[*]=\begin{cases} 1, & \text{if } * \text{ is true} \\ 0, & \text{if } * \text{ is false} \end{cases} \tag{5}$$

For each sensory measurement  $m_i$ , the degree of inconsistency  $I_i$  provides  $l$  distinct range from 0 to  $l$ , If  $m_i$  is more fault than  $m_j$  at the given sample time. The  $I_i$  value of  $m_i$  is smaller than  $I_j$ . Then the estimate value  $\hat{x}$  of the measured parameter is obtained by a weighted average of the remaining measurements at the sample time

$$\hat{x} = \frac{\sum_{i=1}^l m_i I_i}{\sum_{i=1}^l I_i} \tag{6}$$

A flowchart of the redundancy sensory management method is shown in Figure 5. We use the proposed method to detect which measurement value to be faulty. We set the parameter initial values and these initial parameter values contain maximum and minimum value, threshold values,...etc. Then the microchip acquires sensory signals using analogy input interface. Next the microchip calculate the  $I_i$  values using equation ( 4 ),and calculate indicator function values for each sensor using equation ( 5 ). Finally, we can calculate the estimated value using equation (6) for the power detection module.

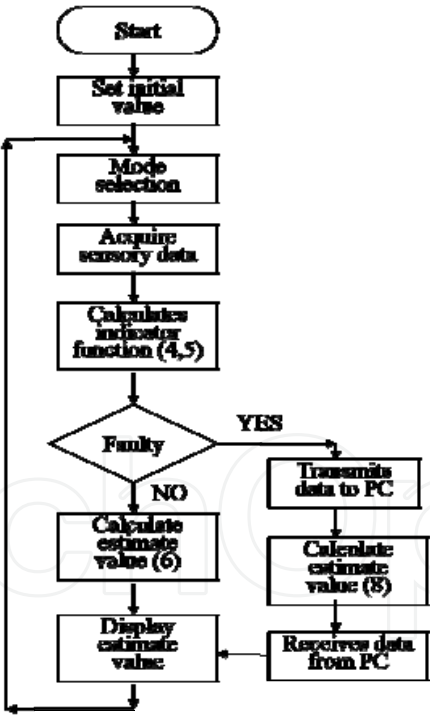


Fig. 5. Flowchart for redundancy sensory management method.

We use redundant sensor management method to detect and diagnose sensory status. When the method is faulty on the  $N+1$  measurement value of the power detection module, we can predict the measurement value using  $P$  estimation value as before. In the chapter, we select  $P$  is 100.

In the level 2, the fusion method is statistical signal perdition method. The fusion decision output of level 1 transmits to main controller (industry personal computer) via series interface (RS232). We model the observed system as the sum of three signal components, to be shown in equation (7).

$$M = X + E \quad (7)$$

If the signal is deterministic and the noise  $E$  is Gaussian with zero mean, then we can calculate the mean value from  $P$  estimated values. The mean value  $\bar{x}$  and standard deviation  $S_i$  is [20]:

$$\bar{x} = \frac{\sum_{k=N-P}^N \hat{x}_i(k)}{P} \quad (8)$$

$$S_i = \sqrt{\frac{1}{P-1} \sum_{k=1}^P (m_i(k) - \hat{x}(k))^2} \quad i = 1, \dots, l \quad (9)$$

Then we use the same  $b_i$  as threshold value, and compute the error between the sensors measured value  $m_i(N+1)$  and mean value  $\bar{x}$ . The error is over the threshold, and we can say the sensor measured value  $m_i(N+1)$  to be faulty. Otherwise, we can say the sensor measured value is exact. That is

$$w_i(N+1) = \begin{cases} 0 & , \quad \left| \frac{m_i(N+1) - \bar{x}}{\bar{x}} \right| \geq 0.05 \\ 1 & , \quad \left| \frac{m_i(N+1) - \bar{x}}{\bar{x}} \right| < 0.05 \end{cases} \quad i = 1, 2, \dots, l \quad (10)$$

$$\hat{x} = \frac{\sum_{i=1}^l w_i(N+1) m_i(N+1)}{\sum_{i=1}^l w_i(N+1)} \quad (11)$$

Finally, we can compute the estimated value of these exact measurement values using equation (11). In the condition, we can say the measurement value of the sensor is faulty. We can not say the sensor to be faulty. That is to say, the proposed method can detect current variety of the mobile robot power system, and isolate the faulty measurement value. But it can not decide the sensor to be broken. We can compute the mean and standard deviation of the each sensor, and compare the standard deviation to decide the broken sensor.

In the redundant management method and statistical signal method, we can get an exact power value for power detection, and isolate faulty signal from current sensor and voltage signal. Then we want to predict the residual power of the mobile robot. First we must fit the curve from the power detection value of the mobile robot. Next the user can set the critical value of the power. The main controller of the mobile robot can calculate the extrapolation value from the critical value, and can calculate the residual working time for the mobile robot.



We fit a second-order polynomial regression

$$y = a_0 + a_1x + a_2x^2 + e \quad (12)$$

The sum of the squares of the error is

$$S_r = \sum_{i=1}^n (y_i - a_0 - a_1x_i - a_2x_i^2)^2 \quad (13)$$

To generate the least squares fit, we take the derivative of Equation (13) with respect to each of the unknown coefficient of the polynomial, and we can get

$$\begin{aligned} na_0 + (\sum x_i)a_1 + (\sum x_i^2)a_2 &= \sum y_i \\ (\sum x_i)a_0 + (\sum x_i^2)a_1 + (\sum x_i^3)a_2 &= \sum x_i y_i \\ (\sum x_i^2)a_0 + (\sum x_i^3)a_1 + (\sum x_i^4)a_2 &= \sum x_i^2 y_i \end{aligned} \quad (14)$$

Finally we can calculate  $a_0, a_1$ , and  $a_2$  from Equation (14). Then we set the power critical value to be  $P_S$  and

$$a_2x^2 + a_1x + a_0 = P_S \quad (15)$$

We can calculate the  $x$  value (the unit is second) from Equation (15). The sample time of the power system is 1 second.

## 6. User Interface

The main controller of the mobile robot is industry personal computer (IPC). The main controller can receive power status of the mobile robot using power detection module. Then the power detection module can transmits four current measured and four voltage measured values, maximum and minimum current values, detection range, detection status, average value and estimate value to the main controller via series interface (RS232). The power detection interface of the mobile robot is shown in Figure 6. The supervised computer can receives measured values from the mobile robot via wireless internet, and display power status of the mobile robot is shown in Figure 7.

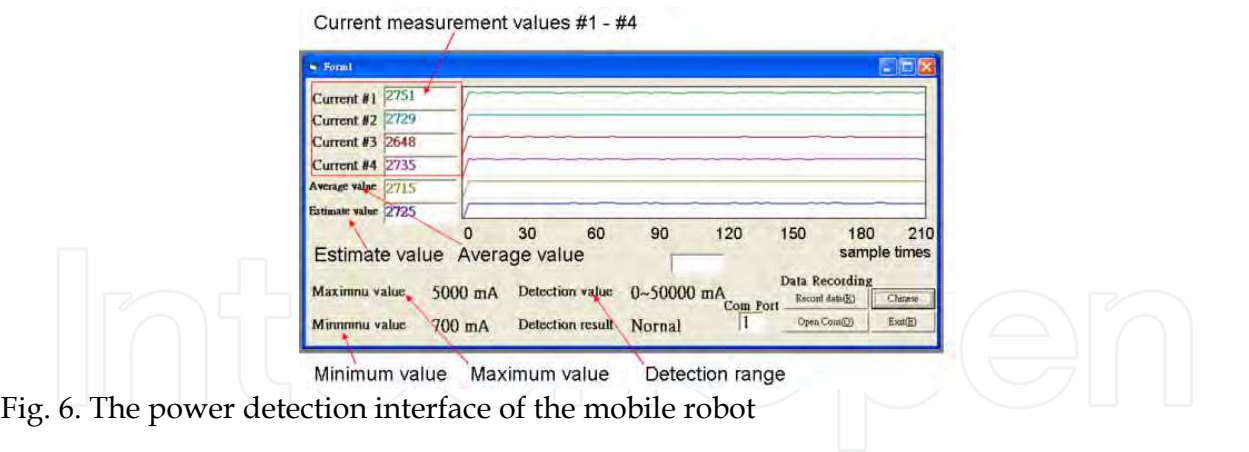


Fig. 6. The power detection interface of the mobile robot

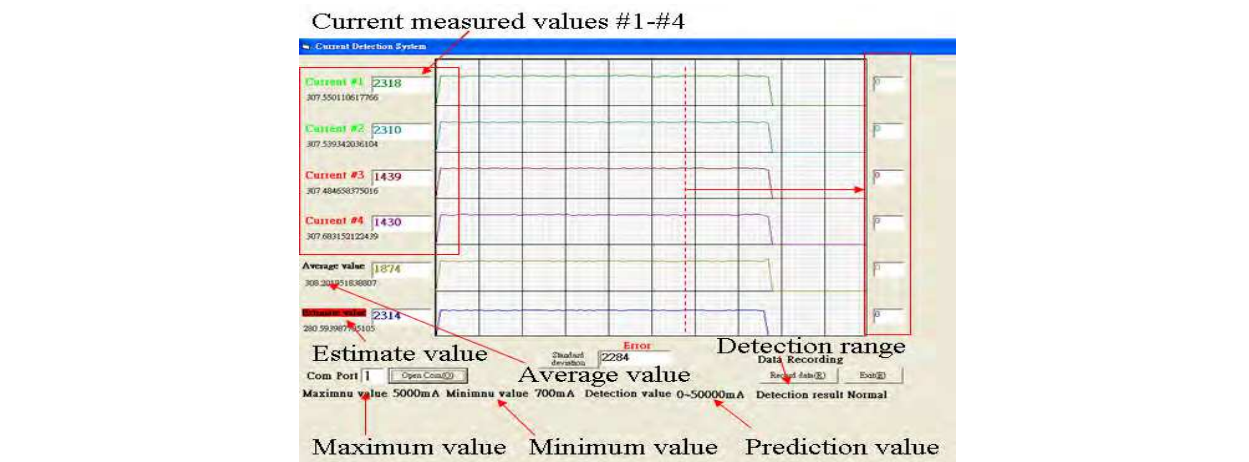


Fig. 7. The power detection interface of the supervised computer

In the monitor, it can display four current, average current and estimation current values on real-time, and plot the curves for these measured values. Users can select any sample time point of these curves using mouse, and display these measured values on the left side of the monitor. It can display the maximum and minimum values, detection range and the standard deviation on the bottom of the monitor.

Another display interface is shown in Figure 8. It can display the standard deviation values on real-time for four current measured values., average measured value and estimated value. It can plot the standard deviation curve for these measurement values. The sample time is one second. The residual power prediction interface of the mobile robot is shown in Figure 9. The upper of the monitor display four current and four voltage measured values, current and voltage average values, and current and voltage estimated values. We plot the curve of power measured value on real-time, and use the proposed method to fit the polynomial curve by the previous one hundred data. Then we set the power critical value to calculate the residual time. It can display on the bottom of the monitor.

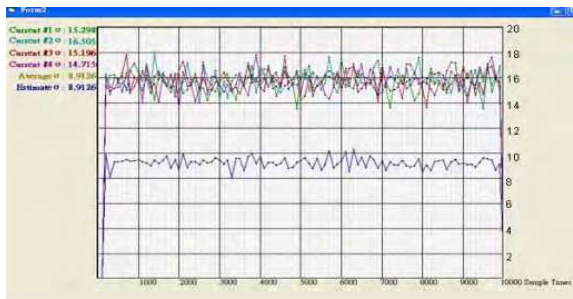


Fig. 8. The standard deviation values for current measurement

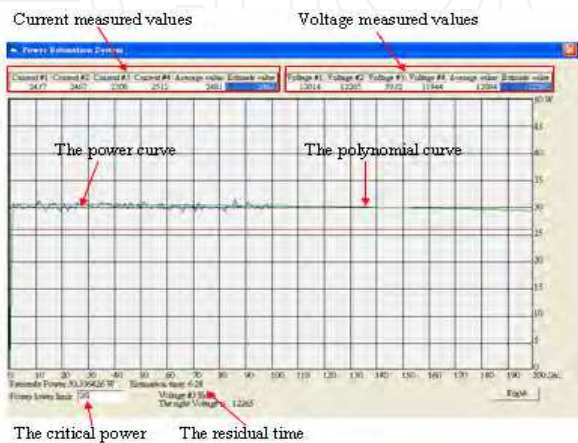


Fig. 9. The residual power prediction

7. Experimental Results

In the power detection system, we use four DC type current sensors to detect the current variety of the mobile robot. The power detection and diagnosis module is equipped in the mobile robot. We test the functions of the power detection module. We can see the module display the current measurement value to be about 9010 mA, and the Amp meter of the mobile robot is 9A. The module can measure the exact current value to be used in the mobile robot, and the experimental result is shown in Figure 10. In the module, we can select the detection mode using switch input to be shown in Figure 11(a). We can select the maximum current is 15A. That is to say, the module must cut off the power output from the power system of the mobile robot, and the power output is over 15A. We can select the minimum current 500mA in the module, too. The power output is small than the minimum current. The module must transmit the signal to mobile robot to find out the recharging station. That is to say, the power of the mobile robot is lack. The experimental is shown is shown in Figure 11(b).



Fig. 10. The power output is about 9 A in the mobile robot



(a)



(b)

Fig. 11. The maximum and minimum current selection mode

Then we use four experiments to implement the diagnosis function of the power detection and diagnosis module, and set the threshold value is 5% of the reference value. In the Figure 12, we pick up the current sensor #1 from the power detection module; we can see the LCD panel display 0mA on the current measurement value. The average value is  $(0\text{mA} + 1470\text{mA} + 1760\text{mA} + 1470\text{mA}) / 4 = 1750\text{mA}$ . The current value is wrong. The exact (estimate) current is  $(1470\text{mA} + 1470\text{mA}) / 2 = 1470\text{mA}$ . The detection value of current sensor #1 is wrong. We must isolate the detection value, and the differential value  $(1470\text{mA} - 0\text{mA})$  is bigger than threshold. The current value (1760mA) of current sensor #3 is wrong, too. We must isolate the detection value (1760mA) that the differential value  $(1760\text{mA} - 1470\text{mA})$  is bigger than threshold.



Fig. 12. The current sensor #1 and #3 are wrong

In the Figure 13, We pick up the current sensor #2, and the measurement value of the sensor #4 is wrong. We can see the LCD panel display 90mA on the current measured value. The average value is  $(2150\text{mA} + 90\text{mA} + 2250\text{mA} + 1860\text{mA}) / 4 = 1587\text{mA}$ . The current value is wrong. The exact (estimate) current is  $(2150\text{mA} + 2250\text{mA}) / 2 = 2100\text{mA}$ . The detection value of current sensor #2 is wrong. We must isolate the detection value for current sensor #2 and #4, and the differential values  $(2150\text{mA} - 90\text{mA})$  and  $(2150\text{mA} - 1860\text{mA})$  are bigger than



threshold. We pick up the current sensor #3, the measurement value is error to be shown in the Figure 14. We can see the LCD panel display 0mA on the power detection module. The average value is  $(1760\text{mA} + 1760\text{mA} + 0\text{mA} + 1660\text{mA})/4 = 1295\text{mA}$ . The current value is wrong. The exact (estimate) current is  $(1760\text{mA} + 1760\text{mA} + 1660\text{mA})/3 = 1726\text{mA}$ . The detection value of current sensor #3 is wrong. We must isolate the detection value for current sensor #3, and the differential value  $(1760\text{mA} - 0\text{mA})$  is bigger than threshold.



Fig. 13. The current sensor #2 and #4 are wrong



Fig. 14. The current sensor #3 is wrong

In the Figure 15, we pick up the current sensor #4, and the measure value of the sensor #3 is wrong. We can see the LCD panel display 90mA. The average value is  $(2050\text{mA} + 2150\text{mA} + 3620\text{mA} + 90\text{mA})/4 = 1977\text{mA}$ . The current value is wrong. The exact (estimate) current is  $(2050\text{mA} + 2150\text{mA})/2 = 2100\text{mA}$ . The detection value of current sensor #4 is wrong. We must isolate the detection value, and the differential value  $(2050\text{mA} - 90\text{mA})$  is bigger than threshold. The current value (1760mA) of current sensor #3 is wrong, too. We must isolate the detection value (3620mA) that the differential value  $(3620\text{mA} - 2050\text{mA})$  is bigger than threshold.



Fig. 15. The current sensor #3 and #4 are wrong

We implement the human machine interface function in the power detection of the mobile robot. The module can transmits the power status and four current measured values to the controller of mobile robot. The experimental scenario is shown in Figure 16. The touch panel can display power status of the mobile robot, and receives four current measured, detection range and maximum and minimum current set values.

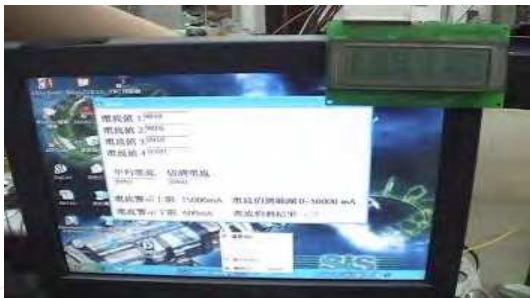


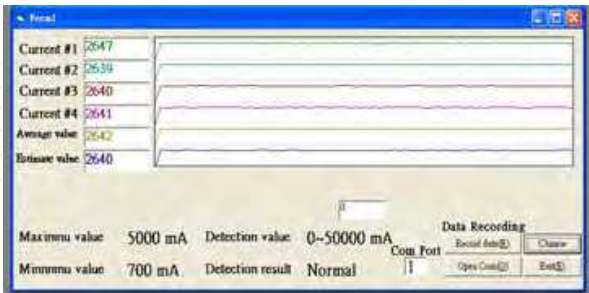
Fig. 16. The interface of mobile robot display the power status

In the current detection and isolation module of the mobile robot, we use four DC type current sensors to detect the current variety for the mobile robot. In the chapter, we assume that a priori of all sensors are the same, and we use computer simulation for four cases. Case I is all sensors are consistent. Case II is one faulty current sensor  $m_4$ . There are three sensors  $m_1, m_2$  and  $m_3$  to be consistent. Case III is two consistent pairs,  $(m_1, m_2)$  and  $(m_3, m_4)$ , that are mutually inconsistent. Case IV presents  $m_1, m_2, m_3$  and  $m_4$  to be mutually inconsistent. The simulation experimental results are shown in [5]. Then we use four experiments to implement the diagnosis function of the current detection and isolation module.

CASE I : If all measurements are consistent, i. e.,  $I_i = 0, i = 1, 2, 3, 4$ , the estimated value is the same as average value, and the estimation value is 2640mA, and we can use the equation (16). The experimental results are shown in Fig. 17. The interface of the mobile robot displays the power status in Figure 17 (a). The interface of the supervised computer displays the power status in Figure 17 (b).

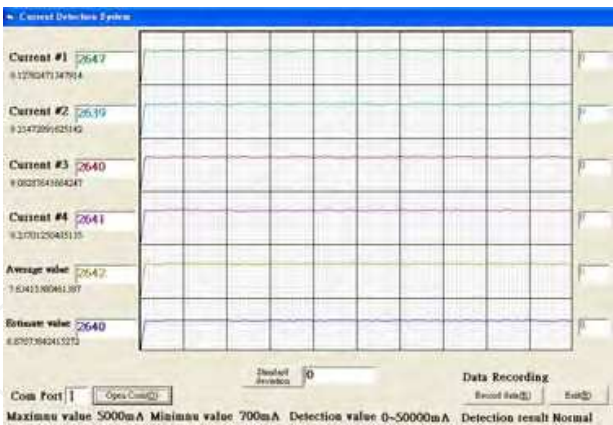
$$\begin{aligned}\hat{x} &= \frac{m_1 w_1 + m_2 w_2 + m_3 w_3 + m_4 w_4}{w_1 + w_2 + w_3 + w_4} \\ &= \frac{2647 + 2639 + 2640 + 2641}{4} \approx 2640\end{aligned}$$

(16)



(a) The display status in the mobile robot





(b) The display status in the supervised computer

Fig. 17. The display status for case I

Case II: The current detection and isolation module has one current sensor to be faulty. We can calculate the  $I_i$  and indicator function as follow

For sensor #1(true) and  $I_1$

$$\left| \frac{2569 \text{ mA} - 2560 \text{ mA}}{2569 \text{ mA}} \right| \leq 0.05 \quad f[*] = 0 \tag{17}$$

$$\left| \frac{2569 \text{ mA} - 2441 \text{ mA}}{2569 \text{ mA}} \right| = 0.049 \leq 0.05 \quad f[*] = 0 \tag{18}$$

$$\left| \frac{2569 \text{ mA} - 22429 \text{ mA}}{2569 \text{ mA}} \right| \geq 0.05 \quad f[*] = 1 \tag{19}$$

$$I_1 = 0 + 0 + 1 = 1 \tag{20}$$

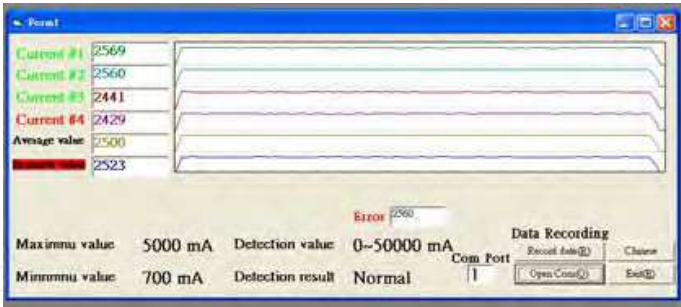
For sensor #4(faulty) and  $I_4$

$$\left| \frac{2429 \text{ mA} - 2569 \text{ mA}}{2420 \text{ mA}} \right| \geq 0.05 \quad f[*] = 1 \tag{21}$$

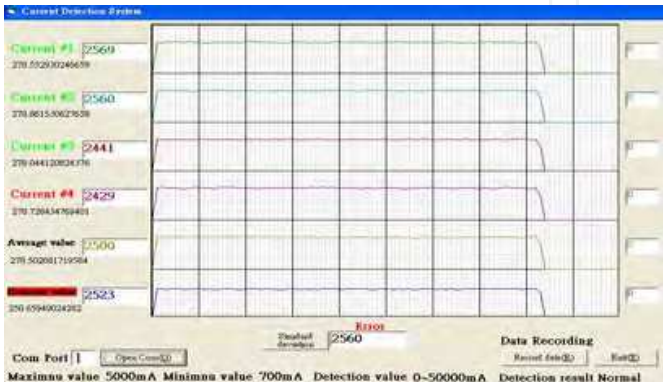
$$\left| \frac{2429 \text{ mA} - 2560 \text{ mA}}{2429 \text{ mA}} \right| = 0.051 \geq 0.05 \quad f[*] = 1 \tag{22}$$

$$\left| \frac{2429 \text{ mA} - 2441 \text{ mA}}{2429 \text{ mA}} \right| \leq 0.05 \quad f[*] = 0 \tag{23}$$

$$I_1 = 1 + 1 + 0 = 2 \tag{24}$$



(a) The display status in the mobile robot



(b) The display status in the supervised computer

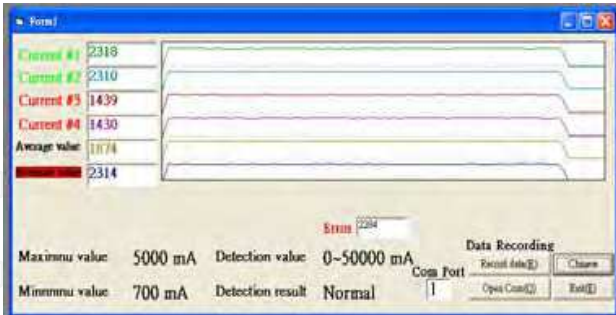
Fig. 18. The display status for case II

We can compute  $I_1 = I_2 = I_3 = 1$ , and  $I_4 = 2$ . We compute the average value  $(2569\text{mA} + 2560\text{mA} + 2441\text{mA} + 2429\text{mA}) / 4 = 2500\text{mA}$  to be wrong. The current value is wrong. The exact (estimate) current is  $(2569\text{mA} + 2560\text{mA} + 2441\text{mA}) / 3 = 2523\text{mA}$ . The detection value of current sensor #4 is wrong. We must isolate the measured value #4. The experimental result is shown in Fig. 18. The estimation value is

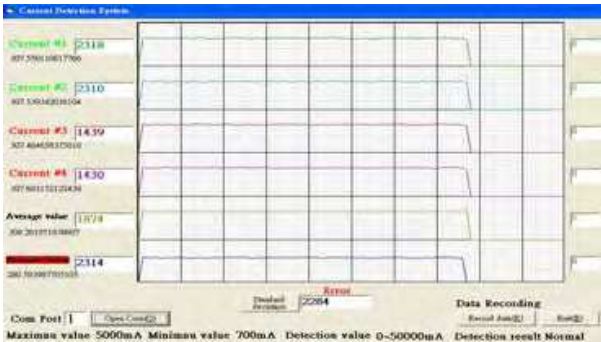
$$\hat{x} = \frac{m_1 w_1 + m_2 w_2 + m_3 w_3}{w_1 + w_2 + w_3} \tag{25}$$

Case III: if two measurements  $m_3$ , and  $m_4$  faulty simultaneously and identically, they are two consistent pairs,  $(m_1, m_2)$  and  $(m_3, m_4)$ , that are mutually inconsistent, and we can fine  $I_1 = I_2 = I_3 = I_4 = 2$ , the result is that no estimate value can be obtained because there is a possible common-mode faulty. That is to say, we can't decide  $(m_1, m_2)$  or  $(m_3, m_4)$ , which pair will be right in the current detection module, and transmits measured values of current sensors to IPC. It can find out faulty sensor using statistical prediction method, and decide an exact estimate value. The experimental result is shown in Fig. 19. The average value is  $(2318\text{mA} + 2310\text{mA} + 1439\text{mA} + 1430\text{mA}) / 4 = 1874\text{mA}$ . The current value is wrong. The current detection and isolation module can not calculate exact (estimate) current. The redundant sensor management method is wrong for the case. We must use statistical signal detection

method to calculate the exact current value for the case. We can compute the mean value is 2284mA, and



(a) The display status in the mobile robot



(b) The display status in the supervised computer

Fig. 19. The display status for case III

$$\left| \frac{2284 \text{ mA} - 1439 \text{ mA}}{2284 \text{ mA}} \right| = 0.37 \geq 0,05 \tag{26}$$

$$\left| \frac{2284 \text{ mA} - 1430 \text{ mA}}{2284 \text{ mA}} \right| = 0.37 \geq 0.05 \tag{27}$$

$$\left| \frac{2284 \text{ mA} - 2318 \text{ mA}}{2284 \text{ mA}} \right| = 0.015 \leq 0.05 \tag{28}$$

$$\left| \frac{2284 \text{ mA} - 2310 \text{ mA}}{2284 \text{ mA}} \right| = 0.013 \leq 0.05 \tag{29}$$

We can say the exact current detection is (2318mA+2310mA)/2=2314mA.  
Case IV: if m1, m2, m3 and m4 are mutually inconsistent, and we can fine I1=I2=I3=I4=3, no estimate value can be obtained because all measurements are inconsistent. That is to say, we can't decide which sensor will be right in the current detection module, and transmits measured values to IPC. It can find out faulty sensor, and decide an exact estimate value. The experimental result is shown in Fig 20. The average value is (2489mA+2219mA+2029mA+2649mA)/4=2347mA. The current value is wrong. The current detection and isolation module can not calculate exact (estimation) current. The redundant sensor management method is wrong for the case. We must use statistical signal detection method to calculate the exact current value for the case. We can compute the mean value is 2198mA, and

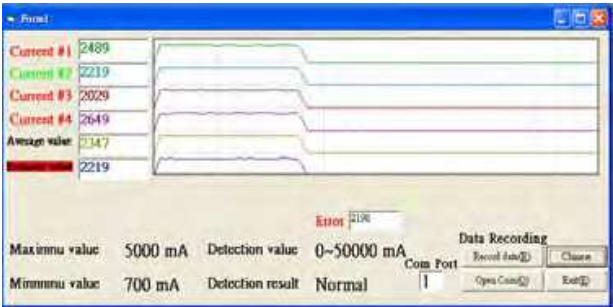
$$\left| \frac{2489\text{ mA} - 2198\text{ mA}}{2198\text{ mA}} \right| = 0.013 \geq 0.05 \tag{30}$$

$$\left| \frac{2219\text{ mA} - 2198\text{ mA}}{2198\text{ mA}} \right| = 0.009 \leq 0.05 \tag{31}$$

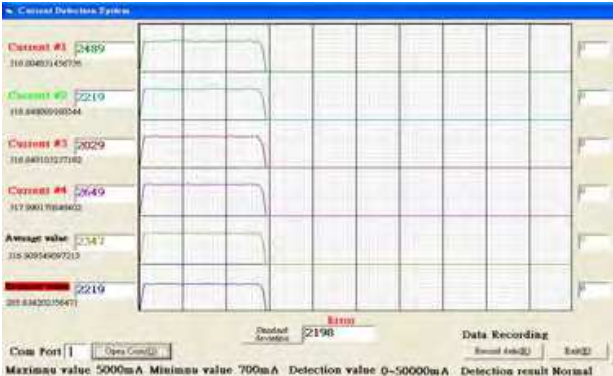
$$\left| \frac{2029\text{ mA} - 2198\text{ mA}}{2198\text{ mA}} \right| = 0.077 \geq 0.05 \tag{32}$$

$$\left| \frac{2649\text{ mA} - 2198\text{ mA}}{2198\text{ mA}} \right| = 0.21 \geq 0.05 \tag{33}$$

We can say the exact current detection is 2219mA.



(a)The display status in the mobile robot



(b) The display status in the supervised computer

Fig. 20. The display status for case IV

In the experimental results of the current sensor diagnosis, we compute the standard deviation of each sensor. If the standard deviation is bigger than threshold, we can say the current sensor to be broken. We must isolate the measured value of the current sensor, and replace it with other current sensor. For case I, all sensors are consistent, and standard deviation varieties of four current sensors are shown in Fig 21. We can see the value is almost 10, and these values are not over threshold.

In the case II, the measured value of current sensor #4 is broken. We can see the standard deviation (145.9) is bigger than threshold. We can diagnose the current sensor #4 to be broken. The experimental result is shown in Fig. 22.



Fig. 21. The standard deviation variety of case I

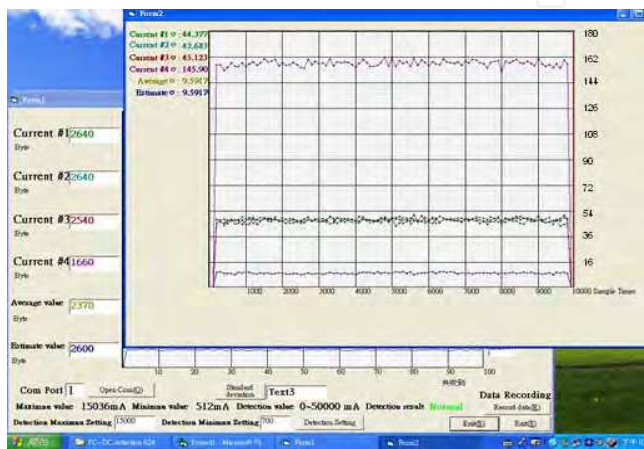


Fig. 22. The standard deviation variety of case II

In the residual power prediction experiment, the user can set the critical power. The proposed method can calculate the residual time, and the power of the mobile robot down to the critical value. In the Fig. 23, the user set the critical power to be 26 W. first, the mobile robot can fit the second-order curve using polynomial regression method. Then it can compute the residual time, display on the bottom of the monitor.

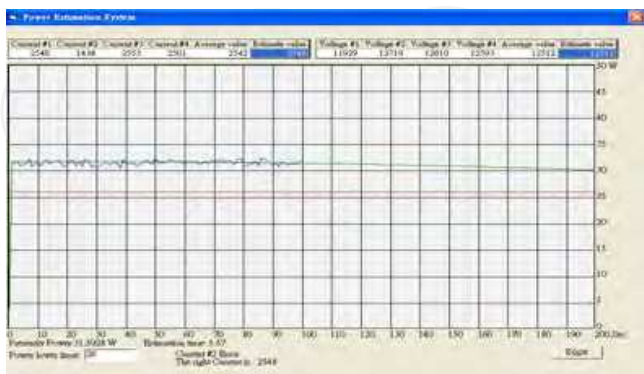


Fig. 23. The residual power prediction for 26W



## 8. Conclusion

We successfully designed a power detection and isolation module that has been integrated in the ISLR-I mobile robot, and calculate the residual power on real-time for the mobile robot. The controller of the power detection and faulty isolation module is HOLTEK microchip. The module can measure maximum current is 50 A, and users can select the current detection range and the detection mode. The detection, isolation and diagnosis algorithm use multilevel multisensor fusion method. There is redundant management method and statistical signal detection method. It can isolate faulty sensor, and estimates an exact power detection value for mobile robot. The module can transmit really current and voltage values, maximum and minimum values, detection range, and detection results to main controller (IPC) of the mobile robot via series interface (RS232). The IPC can transmit the power status to the supervised computer via wireless Internet. The main controller of the mobile robot can fit a second-order polynomial curve using auto-regression method. Then the user can select the critical power value to prediction the residual time on real-time for the mobile robot moving in free space.

## 9. References

- Kuo L. Su , Ting L. Chien and Jr H. Guo, (2004), "Design An Multiagent Based Supervise System Through Internet for Security Robot," The 1nd International Conference on New Technological Innovation for Position, pp.133-138, June 9-11, Congress Center Act city Hamamatsu, Japan.
- Ting L. Chien , Kuo L. Su and Jr H. Guo, (2004), "Develop a Multi Interface Based Detection Module for Home Automation," The 1nd International Conference on New Technological Innovation for Position, pp.289-294.
- Ren C. Lui, Kuo L. Su and Chi W Deng, (2003), "Power Supply Diagnosis System Using Redundant Sensor for Intelligent Security Robot," IEEE International Conference on Industrial Electronic, Control, and Instrumentation, pp.2500-2506.
- H. P. Polenta, A. Ray and J. A. Bernard, (1998), "Microcomputer-based Fault Detection Using Redundant Sensors," IEEE Transactions on Industry Application, Vol.24, No. 5, September/October, pp.905-912.
- Ren C. Luo, Kuo L. Su and Chi W. Deng, (2003), "Multisensor Based Power Supply Diagnosis System for Intelligent Security Robot," IEEE International Conference on Industrial Electronic, Control, and Instrumentation, pp.2500-2506.
- A.J. Melia, (1978), "supply-current analysis (SCAN) as a screen for bipolar integrated circuits," Electronics Letters, Vol.14, No. 14 , pp.434-436.
- G. F. Nelson, W. F. Boggs, (1975), "parametric tests meet the challenge of high\_density ICs," Electronics, Dec. PP108-111.
- M. W. Levi, (1981), "CMOS is most testable," Proceedings of International Test Conference. pp.217-220.
- Y. K. Malaiya, (1984), "Testing stuck-on faults in CMOS integrated circuits", Proceedings of International Conference on Computer-Aided Design, pp.248-250.
- Y. K. Malaiya, S. Y. H. Su, (1982), "A new fault model and testing technique for CMOS devices," Proceedings of International Test Conference, pp.25-34



- J. F. Frenzel, (1994), "Power-Supply Current Diagnosis of VLSI Circuits," IEEE Transaction on reliability Vol. 43, No.1, pp.30-38.
- L. K. Horning et al, (1987), "Measurements of quiescent power supply current for CMOS ICs in production testing", Proceedings of International Test Conference, pp.300-309.
- M. sodden and C. F. Hawkins, (1986), "Test considerations for gate oxide shorts in CMOS ICs", IEEE DEsign & Test, pp.56-64.
- C. Crapuchettes, (1987), "Testing CMOS IDD on large devices," Proceedings of International Test Conference, pp.310-315.
- M. Keating and D. Meyer, (1987), "A new approach to dynamic IDD testing," Proceedings of International Test Conference, pp.316-321.
- L. R. Carley and W. Maly, (1988), "A circuit breaker for redundant IC systems, Proceedings of Custom Integrated Circuits Conference, pp.27.6.1-27.6.6.
- W. Maly and P. Nigh, (1988), "Build-in current testing- Feasibility study," Proceedings of International Conference on Computer-Aided Design, pp.340-343.
- Kuo L. Su, (2006), "Automatic Fire Detection System Using Adaptive Fusion Algorithm for Fire Fighting Robot," IEEE International Conference on System, Man and Cybernetics, Grand Hotel, Taipei, Taiwan, October 2006, pp.966-971.
- Kuo L. Su, Ting L. Chien and Jr H. Guo, (2004), "Design a Low Cost Security Robot Applying in Family," International Conference on Autonomous Robots and Agents, December 13-15, Palmerston North, NZ, pp.367-372.
- Kuo L. Su, Ting L. Chien and Jr H. Guo, (2005), "Decelop a Seft-diagnosis Function Auto-recharging Device for Mobile Robot," IEEE International Workshop on Safety, Security, and Rescue Robot, pp.1-6.

IntechOpen



## **Mechatronic Systems Applications**

Edited by Annalisa Milella Donato Di Paola and Grazia Cicirelli

ISBN 978-953-307-040-7

Hard cover, 352 pages

**Publisher** InTech

**Published online** 01, March, 2010

**Published in print edition** March, 2010

Mechatronics, the synergistic blend of mechanics, electronics, and computer science, has evolved over the past twenty five years, leading to a novel stage of engineering design. By integrating the best design practices with the most advanced technologies, mechatronics aims at realizing high-quality products, guaranteeing at the same time a substantial reduction of time and costs of manufacturing. Mechatronic systems are manifold and range from machine components, motion generators, and power producing machines to more complex devices, such as robotic systems and transportation vehicles. With its twenty chapters, which collect contributions from many researchers worldwide, this book provides an excellent survey of recent work in the field of mechatronics with applications in various fields, like robotics, medical and assistive technology, human-machine interaction, unmanned vehicles, manufacturing, and education. We would like to thank all the authors who have invested a great deal of time to write such interesting chapters, which we are sure will be valuable to the readers. Chapters 1 to 6 deal with applications of mechatronics for the development of robotic systems. Medical and assistive technologies and human-machine interaction systems are the topic of chapters 7 to 13. Chapters 14 and 15 concern mechatronic systems for autonomous vehicles. Chapters 16-19 deal with mechatronics in manufacturing contexts. Chapter 20 concludes the book, describing a method for the installation of mechatronics education in schools.

### **How to reference**

In order to correctly reference this scholarly work, feel free to copy and paste the following:

Kuo-Lan Su, Jr-Hung Guo and Jheng-Shiann Jhuang (2010). Develop a Power Detection and Diagnosis Module for Mobile Robots, *Mechatronic Systems Applications*, Annalisa Milella Donato Di Paola and Grazia Cicirelli (Ed.), ISBN: 978-953-307-040-7, InTech, Available from:

<http://www.intechopen.com/books/mechatronic-systems-applications/develop-a-power-detection-and-diagnosis-module-for-mobile-robots>

**INTECH**  
open science | open minds

### **InTech Europe**

University Campus STeP Ri  
Slavka Krautzeka 83/A  
51000 Rijeka, Croatia  
Phone: +385 (51) 770 447

### **InTech China**

Unit 405, Office Block, Hotel Equatorial Shanghai  
No.65, Yan An Road (West), Shanghai, 200040, China  
中国上海市延安西路65号上海国际贵都大饭店办公楼405单元  
Phone: +86-21-62489820

[www.intechopen.com](http://www.intechopen.com)

Fax: +385 (51) 686 166  
www.intechopen.com

Fax: +86-21-62489821

IntechOpen

IntechOpen

© 2010 The Author(s). Licensee IntechOpen. This chapter is distributed under the terms of the [Creative Commons Attribution-NonCommercial-ShareAlike-3.0 License](https://creativecommons.org/licenses/by-nc-sa/3.0/), which permits use, distribution and reproduction for non-commercial purposes, provided the original is properly cited and derivative works building on this content are distributed under the same license.

IntechOpen

IntechOpen